Available online at www.sciencedirect.com
ScienceDirect
Trans. Nonferrous Met. Soc. China 32(2022) 2877−2888
Transactions of Nonferrous Metals Society of China
www.tnmsc.cn

Evolution of microstructure and mechanical properties of ZK60 magnesium alloy processed by asymmetric lowered-temperature rolling

Wen-cong ZHANG, Xin-tong LIU, Jun-fei MA, Wen-ke WANG, Wen-zhen CHEN, Yu-xuan LIU, Jian-lei YANG

School of Materials Science and Engineering, Harbin Institute of Technology, Weihai 264209, China

Received 2 November 2021; accepted 7 June 2022

Abstract: Asymmetric lowered-temperature rolling was applied to the fabrication of fine-grained ZK60 magnesium alloy sheet with weak basal texture along the rolling direction (RD). The results showed that multi-pass lowered-temperature rolling could significantly improve the microstructure homogeneity and refine the grain size. Meanwhile, a fiber texture along the transverse direction (TD) gradually developed during rolling process. Importantly, the shear deformation along the RD made the *c*-axis of basal plane rotate to the RD, weakening the basal texture along this direction. Influenced by such microstructure variation, the yield strength along the TD continuously increased due to the successive grain refinement and the increased activation of prismatic slips, whereas the uniform elongation decreased owing to the decline of strain hardening ability. In contrast, the continuous weakening of basal texture along the RD increased the activation of soft basal slips, greatly offsetting the strengthening effect contributed by grain refinement and thereby causing the slight decrease of yield strength.

Key words: rolling; asymmetric rolling; grain size; texture; yield stress

1 Introduction

Magnesium alloys have become necessary materials for aerospace and transportation because of their low density, high specific strength and good stiffness [1,2]. However, the inherent hexagonal close packed (hcp) structure of magnesium alloys generally resulted in poor ductility and sheet formability, which severely limited their engineering applications [3,4]. In fact, the addition of rare earth elements to weaken the basal texture has been used to effectively improve the formability of the sheets [5−7]. However, the addition of expensive rare earth elements seriously increased the cost, which led to a negative impact on industrial production. Therefore, many researchers have controlled the average grain size and the basal texture by plastic processing techniques to obtain sheets with good ductility, such as equal channel angular pressing (ECAP), and repeated unidirectional bending (RUB). It was reported that AZ91 magnesium alloy with a fine grain size of 5 μm was fabricated by ECAP and its elongation increased from 5% to 18% [8]. In terms of texture, the basal texture intensity of AZ31 magnesium alloy sheets was weakened from 10.7 to 6.3 via RUB, thereby improving the Erichsen value of sheets from 5.5 to 7.5 [9]. Compared with these plastic process techniques, asymmetric rolling not only refined the grain and weakened the basal texture by introducing shear strain, but also had high production efficiency. Typically, AZ31 basal texture was weakened from 8.7 to 7.5 by DSR [10]. The grain size of AZ31 was refined to 1.5 μm and the elongation was increased to 35% by asynchronous rolling [11]. GONG et al [12] reported more significant weakening of the basal texture as the velocity ratio increased during rolling. CHANG et al [13] fabricated AM31 magnesium

Corresponding author: Wen-ke WANG, Tel/Fax: +86-631-5672167, E-mail: 15B309020@hit.edu.cn
DOI: 10.1016/S1003-6326(22)65990-9

alloy sheets with a fine grain size of 4.9 μm via the asymmetric rolling. Indeed, the principle of grain refinement by DSR was based on the Zener−Hollomon parameter Z ($Z=\dot{\varepsilon}\exp[Q/(RT)]$), where $\dot{\varepsilon}$ is the strain rate, T is the deformation temperature, Q is the activation energy and R is the molar gas constant. It can be noted that the lower deformation temperature was beneficial to refining the grains. The grain size of ZK60 alloy was refined from 26.9 to 5.2 μm by multi-pass lowered-temperature rolling [14]. Thus, introducing the lowered-temperature method into the DSR will improve the grain refinement ability. Crucially, the lowered temperature increased the degree of basal slip involvement and enhanced the adjustment of shear strain on the texture. However, there were very few research on this aspect. In this work, the multi-pass asymmetric lowered-temperature rolling was applied to ZK60 magnesium alloy sheets to achieve sufficient grain refinement and texture adjustment. The evolution of microstructure and mechanical properties was analyzed. Moreover, the effect of microstructure on the mechanical properties was investigated in combination with the strain hardening curves.

2 Experimental

The initial materials in this work were hot-extruded ZK60 (Mg−6.63wt.%Zn−0.56wt.%Zr) alloy sheets with the thickness of 10 mm. And the initial sheets for this work were supplied by Yueyang Yuhang Co. (China). It is reported that the ratio of upper-to-lower roll speed was an important rolling parameter in asymmetric rolling. In this work, the diameters of the upper and lower rolls were identical and the ratio of upper-to-lower roll speed was set to be 1.2:1. And the speed of slow roll was 18 m/min. All the sheets were preheated to 623 K for 40 min prior to rolling, and then rolled from 10 to 2.1 mm in the thickness by 3 passes with the thickness reduction of 40% per pass. The deformation temperature gradually decreased from 623 to 573 K during the rolling process. The rolling process parameters are given in Table 1. The temperature was measured using contact thermometry, and the sheets were cooled down in air.

The specimens for tension were designed with a diameter of 15 mm in gauge, as shown in Fig. 1. Before the tensile test, the specimens were sandpapered to remove surface defects such as pits and scratches. The mechanical properties were tested by Instron 5569 machine with a strain rate 6.7×10^{-4} s^{-1} at room temperature.

Table 1 Asymmetric lowered-temperature rolling parameters for ZK60 magnesium alloys

Pass No.	Temperature/ K	Thickness variation/mm	Thickness reduction/%
1	623	10→6	40
2	598	6→3.6	40
3	573	3.6→2.1	40

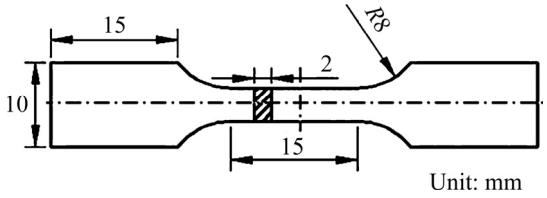

Fig. 1 Size of tension samples

Microstructure characteristics were examined on the RD−TD sheet plane (ED: extrusion direction, RD: rolling direction, and TD: transverse direction). Electron backscattering diffraction (EBSD) was performed on ZEISS MERLIN Compact to obtain the microstructure and texture. Specimens for EBSD were prepared by mechanical polishing, followed by electropolishing in the solution of C_2H_5OH and H_3PO_4 with volume ratio of 5:3 for 8 min at 0.25 A. In order to obtain a high-quality texture, an accelerating voltage of 20 keV, and a working distance of 15 mm with a sample tilt angle of 70° were selected. To ensure reproducible results, three experiments were performed for each condition.

3 Results and discussion

3.1 Microstructure characteristics

The microstructure characteristics of the initial material and the rolled sheets are shown in Fig. 2, and their grain size distributions are summarized in Fig. 3. Figures 2(a, c, e, g) show twin boundary distribution maps in the rolling process, and Figs. 2(b, d, f, g) show grain orientation spread (GOS) maps of the selected areas. The average misorientation of each individual measurement point within the grain determines the GOS. Greater

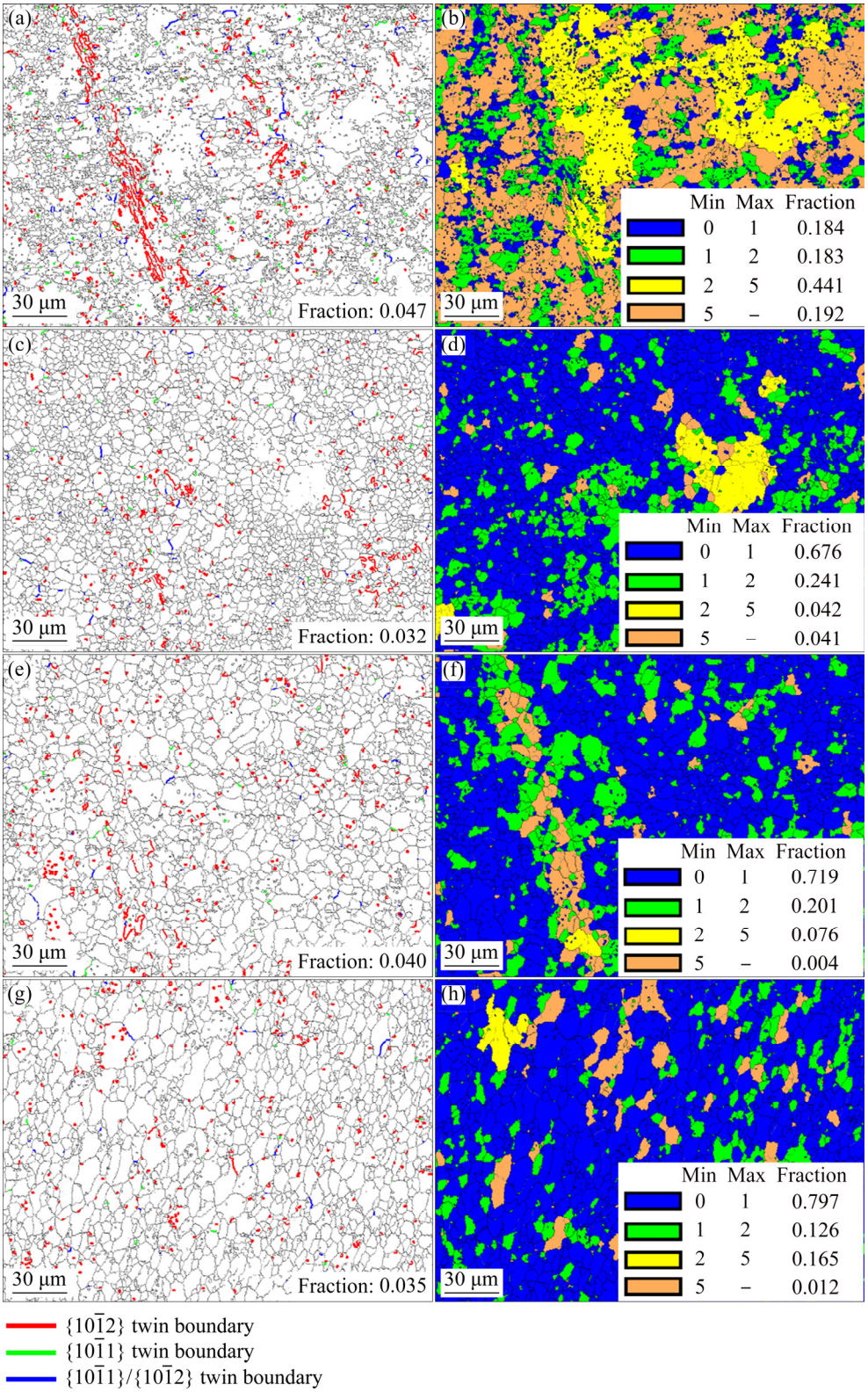

Fig. 2 Twin boundary distribution maps in rolling process (a, c, e, g) and grain orientation spread (GOS) maps (b, d, f, h) of selected areas: (a, b) Initial; (c, d) Pass 1; (e, f) Pass 2; (g, h) Pass 3

GOS value means more deformation in a grain. In this work, dynamic recrystallized grains were identified by GOS values smaller than 2° (blue and green colored grains), while those of the deformed grains were greater than 2° (orange and yellow colored grains). As shown in Fig. 2(b), the initial microstructure was a typical duplex crystal. Many fine grains were distributed on the grain boundaries

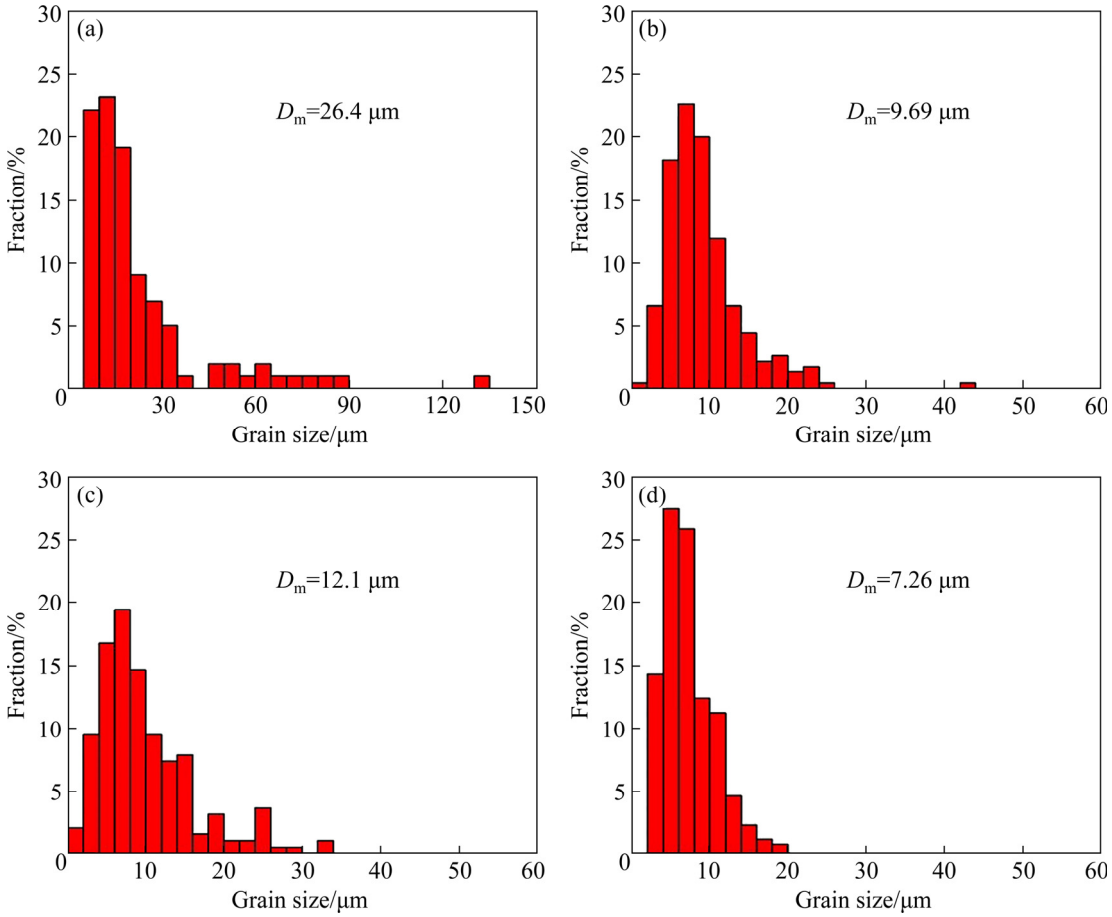

Fig. 3 Grain size distributions for ZK60 magnesium alloy sheets during asymmetric lowered-temperature rolling: (a) Initial; (b) Pass 1; (c) Pass 2; (d) Pass 3

of deformed coarse grains, and twins occurred in some of the coarse grains. The percentage of fine grains in the initial material was 37%. In addition, the grain size of the initial sheet was 5.2−133.5 μm, which indicated that the microstructure of the initial material with an average grain size of 26.4 μm was poorly uniform.

After the first pass, the average grain size was refined to 9.69 μm. A large number of equiaxed fine grains appeared in the microstructure, but there were still many coarse grains. The percentage of dynamic recrystallization grains (DRX) increased from 37% to 92% after rolling from Fig. 2. The results suggested that DRX occurred partially in Pass 1. However, compared with the initial material, the percentage of DRX grains increased significantly, which was beneficial to the homogeneity of microstructure. As the rolling proceeded and the temperature was lowered, DRX occurred again in Pass 2, and more fine equiaxed grains appeared. The percentage of fine grains was also increased. The number of coarse grains was significantly reduced. Finally, a nearly uniform microstructure with an average grain size of 7.26 μm was obtained after the third pass at 573 K. The coarse grains in Pass 3 were nearly eliminated. The results showed that the multiple DRX during current multi-pass varied-speed rolling process not only refined the microstructure, but also improved the uniformity of the microstructure.

It can be seen that the content of twins was increased in Pass 2 compared with Pass 1, as shown in Figs. 2(a, c). This was related to the thickness reduction and deformation speed in the rolling process. The twin nucleation was not a thermally activated process, but a stress activated process. The thickness reduction of 40% per pass caused a relatively large stress concentration near the grain boundaries during rolling, which promoted the formation of twins. On the other hand, the experimental rolling speed of 18 m/min led to a higher strain rate, while the deformation mechanisms mainly controlled by the speed such as cross-slip or grain boundary slip could not be

activated in time. Thus, it also led to the local stress concentration near the grain boundaries and promoted twin nucleation. Moreover, the twin accumulation in Pass 1 and Pass 2 provided nucleation sites for the DRX in Pass 3, resulting in a more complete DRX in Pass 3 [15].

3.2 Texture characteristics

Figure 4 shows the (0002), $(10\bar{1}0)$, $(11\bar{2}0)$ pole figures of ZK60 magnesium alloy sheets. Clearly, the (0002) basal plane in the initial material was nearly parallel to the ED−ND plane with the maximal intensity of 18. It can also be seen that the $(10\bar{1}0)$ and $(11\bar{2}0)$ crystal planes were symmetrical about the TD, which were similar to the $(11\bar{2}0)\langle 10\bar{1}0\rangle$ texture of the magnesium single crystals (Fig. 4(a)). After the first pass, the (0002) pole figure exhibited a fiber texture, implying that *c*-axis of the grains transformed from being parallel to TD to diffusely distributing along the TD. Due to the normal pressure, a strengthening zone appeared in the center of the (0002) pole figure, and the intensity was decreased to 5.9. In addition, the $(10\bar{1}0)$ and $(11\bar{2}0)$ pole figures in initial material transformed into hexagonally symmetric structure, which was caused by plastic deformation [16,17]. As rolling proceeded, the (0002) pole figure showed that the *c*-axis was still diffusely distributed along the TD, and there was also a strengthening zone in the $(10\bar{1}0)$ pole figures along the RD (Fig. 4(c)). However, $(11\bar{2}0)$ pole figure showed a strengthening zone parallel to the RD, which indicated the formation of recrystallized texture components. The result suggested that DRX occurred significantly, corresponding to the above analysis (Fig. 2(b)) [17]. Finally, the (0002) pole figure of Pass 3 showed that the distribution of the *c*-axis was slightly more concentrated along the TD than that of Pass 2, with a rotation along the RD. This indicated that rotation occurred in (0002) basal

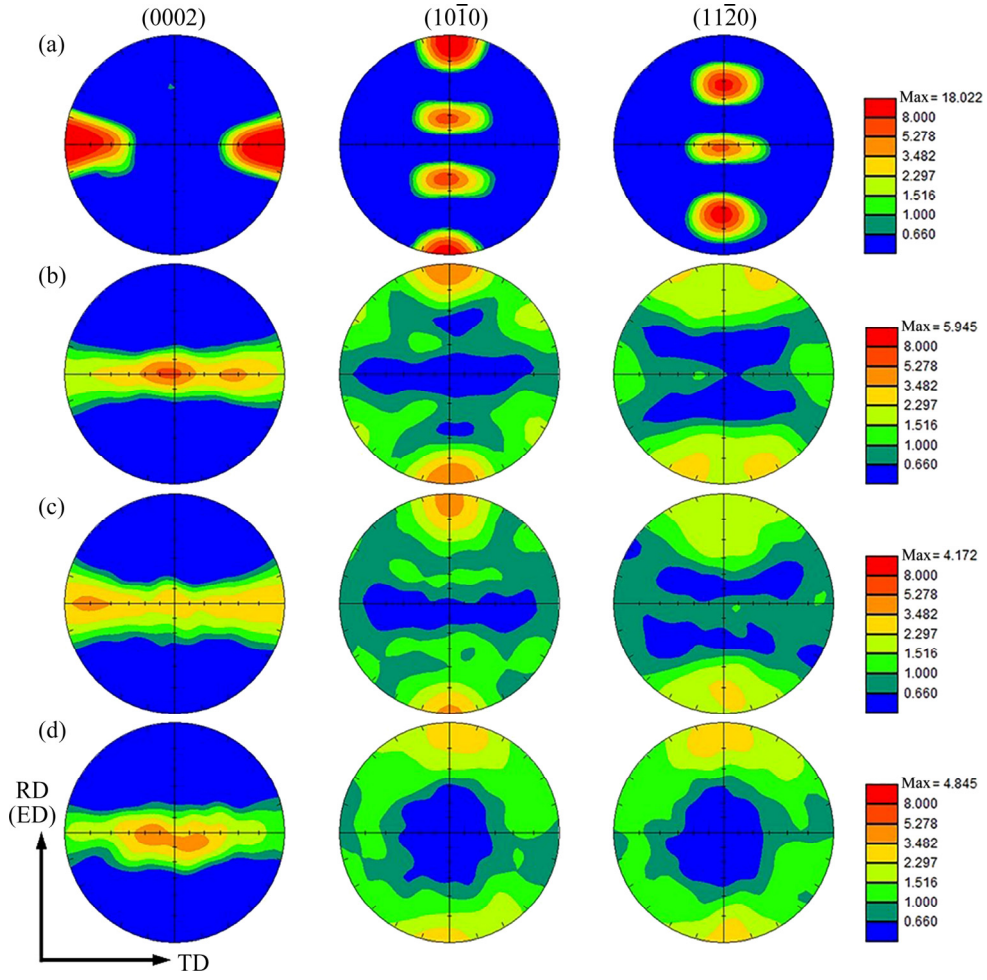

Fig. 4 (0002), $(10\bar{1}0)$ and $(11\bar{2}0)$ pole figures of ZK60 magnesium alloy sheets during asymmetric lowered-temperature rolling: (a) Initial; (b) Pass 1; (c) Pass 2; (d) Pass 3

plane along the RD due to the introduction of shear deformation by asymmetric lowered-temperature rolling. The previous microstructure results showed that the DRX was more complete in Pass 3, and the recrystallization texture component caused a strengthening zone parallel to the RD in the $(11\bar{2}0)$ pole figure.

In this work, to further demonstrate the grain rotation in the rolling process, normalized (0002) pole density intensity distribution was given, as shown in Fig. 4. The (0002)-times random along the RD was taken from pole figure. The data were subjected to normalization processing in which the values of time random were divided by $\int_0^{\pi/2} I\cos\theta \mathrm{d}\theta$ (I is the intensity and θ is the angle away from RD) to get normalized pole density distribution. As shown in Fig. 5, the angle in the figure represented the angle between the *c*-axis and the RD or TD, while the pole density value larger than 1.5 was taken as the reference value of preferred orientation. Clearly, the (0002) basal pole density distributions between the RD and the TD in the initial material showed a distinct difference. The initial material exhibited a very significant preferred orientation of the (0002) pole density along the RD, with the maximum pole density value of 21.3 in the angle range of 81°−90° (Fig. 5(a)). Compared with the RD, the preferred orientation along the TD was in the range of 0.6°−30°, with the maximum pole density of 4.46. Additionally, the (0002) pole density distribution along the RD showed that the maximum pole density value gradually decreased with rolling, which were 9 (Pass 1), 7.1 (Pass 2) and 6.1 (Pass 3). And the (0002) pole density distribution of the rolled sheets was more diffusive compared with the initial material, and the range of the preferred orientation angle gradually expanded with the increased of passes to 71°−90° (Pass 1), 67°−90° (Pass 2) and 65°−90° (Pass 3). These results showed that asymmetric lowered-temperature rolling led to the (0002) basal plane more diffusively distributed along the RD by introducing shear deformation, which effectively weakened basal texture along the RD. It can also be seen that the weakening effect of the basal texture was the most obvious in Pass 1 and gradually decreased with increasing passes (Fig. 5(a)). Compared with the initial material, the (0002) basal pole density distributions of the rolled sheet were completely diffusive along the TD and the maximum pole density values were significantly lowered, 2.25 (Pass 1), 1.77 (Pass 2) and 2.53 (Pass 3). In general, both the concentration of the preferred orientation range and the maximum pole density values of the basal texture intensity along the RD were higher than those along the TD, and the reason was mainly related to the obvious difference in the texture of the initial material along the RD and TD.

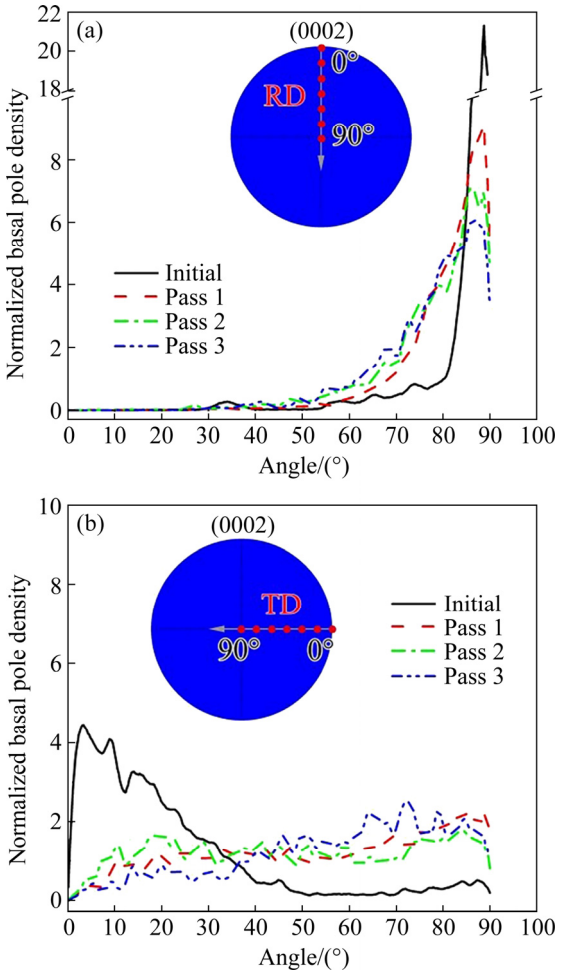

Fig. 5 (0002) pole density distributions of ZK60 magnesium alloy sheets during asymmetric lowered-temperature rolling: (a) RD; (b) TD

It is notable that the maximum pole density values and the angle ranges of the preferred orientation were less different along the TD of all the rolled sheets, which may be related to the higher deformation temperature and fewer passes during the rolling process. The deformation temperatures in this work were all higher than 300 °C. As reported, the critical resolved shear stress (CRSS) for non-basal slip is markedly lower at this temperature, which meant that the activation of

non-basal slip was increased. This ultimately led to a reduction in the percentage of basal slip involved in deformation [18,19]. This means that the propensity of the (0002) basal plane to turn toward the RD−TD plane during the rolling process was weakened, resulting in a weakened texture along the TD. In fact, although the CRSS of non-basal slip decreased at high temperature and the percentage of activation increased significantly, the CRSS values of non-basal slip were still higher than those of basal slip at this time, indicating that basal slip was still the dominant deformation mechanism. In rolling process, the basal plane would gradually turn to the RD−TD plane due to the pulling and normal force along the RD. However, due to the fewer passes, the basal slip exerted less and the accumulation of basal plane turned to RD−TD plane was insufficient, resulting in a weakened basal texture. Above analyses indicated that higher deformation temperatures and fewer rolling passes were conducive to slowing down the tendency of the basal plane to rotate to the RD−TD plane.

3.3 Mechanical properties

Figure 6 shows the comparison of the measured stress−strain responses of ZK60 magnesium alloy sheets during asymmetric lowered-temperature rolling. The variations of mechanical properties are shown in Table 2 and Fig. 7. The yield strength (YS) along the TD gradually increased from 157 MPa (initial material) to 216 MPa (Pass 3) with the rolling process. But the YS varied less along the RD, remaining between 236 and 251 MPa (Table 2). In fact, the variation of YS was influenced by average grain size and texture. The YS gradually increased along the TD due to the effect of grain refinement and basal texture strengthening. However, the continuous weakening of basal texture along RD increased the activation fraction of soft basal slips, greatly offsetting the strengthening effect contributed by grain refinement and thereby causing the slight decrease in yield strength. Figure 6 also showed that the variation of ultimate tensile strength (UTS) along the TD and RD was not distinct, indicating that the UTS was less sensitive to grain size and texture than the YS.

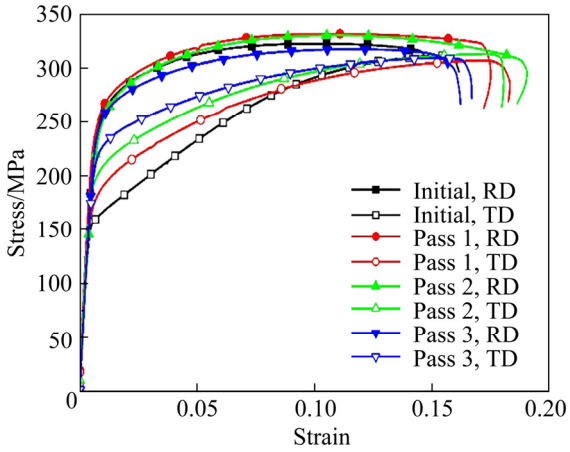

Fig. 6 Stress−strain curves of ZK60 magnesium alloy sheets during asymmetric lowered-temperature rolling

In order to analyze the above variation of yield strength (Fig. 7(a)), this work applied the orientation distribution maps to characterize the deformation modes, as shown in Fig. 8. As reported, the mechanical properties were closely related to the deformation modes. The activation of the deformation mode was depended on the CRSS and the Schmidt factor ($\sigma_0=\tau_c/m$, where σ_0 was the friction stress for dislocation movement, τ_c represented the critical resolved shear stress and m represented the Schmid factor, respectively). The deformation temperature of the magnesium alloy was the main factor influencing the CRSS. In this work, the temperature was constant during tension and therefore the value of the CRSS was invariant for each deformation mode. On the other hand, the Schmid factor was related to the relative

Table 2 Mechanical properties of ZK60 magnesium alloy sheets during asymmetric lowered-temperature rolling

Sample	YS/MPa		UTS/MPa		UE/%		FE/%	
	RD	TD	RD	TD	RD	TD	RD	TD
Initial	251±4	157±3	322±4	311±3	10.1±0.3	15.3±0.4	14.6±0.3	16.1±0.4
Pass 1	245±3	175±1	331±5	307±2	10.7±0.1	17.2±0.2	17.5±0.3	18.3±0.3
Pass 2	236±2	193±3	330±3	313±3	10.7±0.3	17.2±0.3	19.1±0.4	18±0.4
Pass 3	241±2	216±4	317±4	309±4	12±0.2	15.3±0.3	16.3±0.4	16.7±0.3

YS—Yield strength; UTS—Ultimate tensile strength; UE—Uniform elongation; FE—Fracture elongation

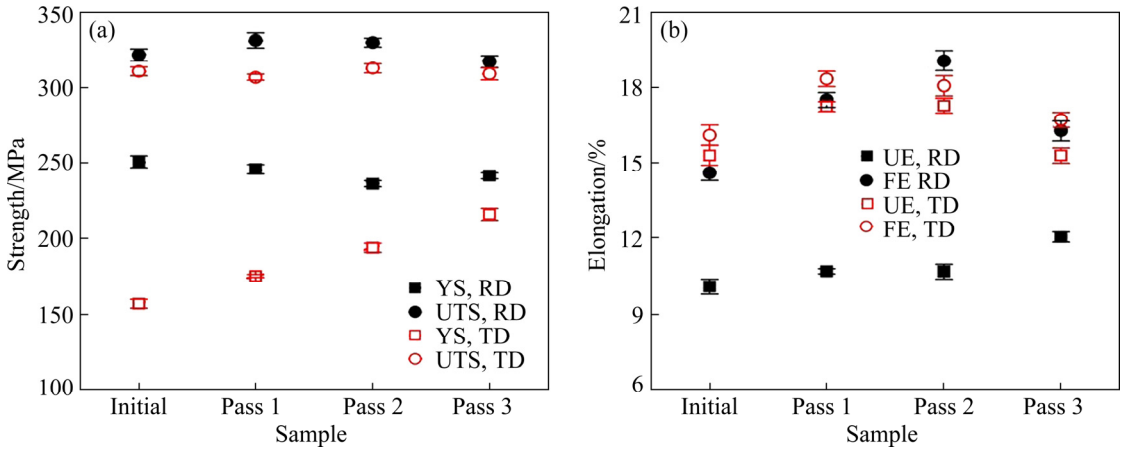

Fig. 7 Variations of mechanical properties of ZK60 magnesium alloy sheets during asymmetric lowered-temperature rolling: (a) Yield strength (YS) and ultimate tensile strength (UTS); (b) Uniform elongation (UE) and fracture elongation (FE)

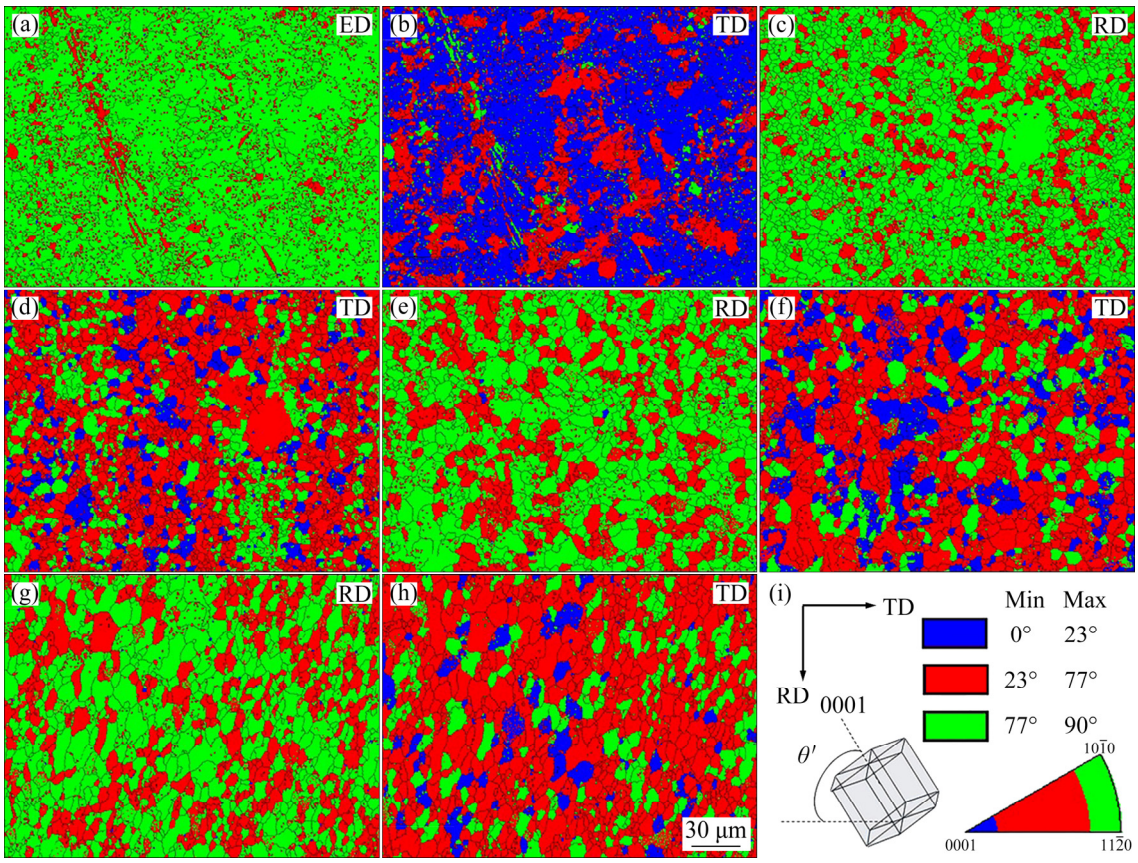

Fig. 8 Orientation distributions of ZK60 alloys using grain orientation maps: (a, b) Initial material; (c, d) Pass 1; (e, f) Pass 2; (g, h) Pass 3 (In grain orientation map, the grains with the ⟨0001⟩ away from the tension direction in the angle ranges of 0°−23°, 23°−77° and 77°−90° were depicted by blue color, red color and green color, respectively)

relationship between tensile directions. Thus, the crystal orientation was the only variable affecting the deformation mode of the alloy when the direction of tension was constant. Therefore, in this work, the orientation distribution of the alloy was obtained using grain orientation maps (Fig. 8). The associated activation fraction of each deformation mode was calculated, as shown in Fig. 9. According to the study, when the CRSS ratio of basal slip, tensile twinning and prismatic slip was set to be

1:1:2, the dominant deformation modes were tensile twinning with θ'=0°−23°, basal slip with θ'=23°−77° and prismatic slip with θ'=77°−90° (θ' was the angle between the direction of tension and the direction normal to the base plane) [20]. In this work, the deformation mode during the tensile test was characterized by selecting the tensile direction (ED or TD) as the sample direction and the ⟨0001⟩ direction as the crystal direction. And tensile twinning, basal slip and prismatic slip were highlighted in blue, red and green, respectively.

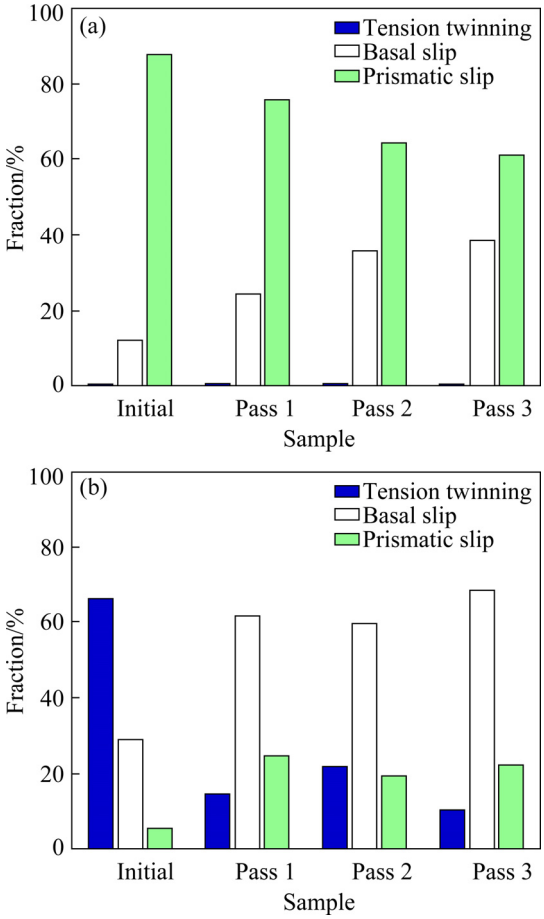

Fig. 9 Activation fractions of each deformation mode during tension tests along RD (a) and TD (b) based on orientation distributions in Fig. 8

Figures 8(a, b) show orientation distribution of the initial material, which consisted mainly of 77°−90° grains with minor supplement 0°−23° grains along the ED. Compared to the ED, 23°−77° grains and 0°−23° grains appeared along the TD, which was identified with tensile twinning of 65.8% and basal slip of 65.8% in Fig. 9(b). That was to say, the initial material deformation mode was mainly prismatic slip along the ED, and was mainly tensile twinning along the TD, with minor basal slip and prismatic slip as supplement. After the first pass, the 0°−23° grains increased along the RD, but along the TD, the 23°−77° grains decreased obviously. The 0°−23° grains and 77°−90° grains increased along the TD, corresponding with the results in Fig. 9(b). Eventually, 0°−23° grains increased to 38.6% and 77°−90° grains decreased to 61.2% along the RD. Along the TD, 23°−77° grains decreased to 9.9%, with 0°−23° grains of 68.2% and 77°−90° grains of 21.9%. In general, as rolling proceeded, prismatic slip gradually decreased but basal slip gradually increased along the RD. Along the TD, tensile twinning decreased noticeably; however, basal slip and prismatic slip increased.

Different texture produced the activation of different deformation modes, which in turn had an effect on the mechanical properties. Obviously, the yield stress decreased with the increased activation of basal slip along the RD (ED). And the yield stress gradually decreased with the decrease of activation of prismatic slip, which was in agreement with the results in the reference [21]. Along the TD, the yield stress of the initial material was low due to the large activation of the initial material tensile twinning. Due to the increase in prismatic slip and the notable reduction in tensile twinning, the yield strength showed a gradual increase along the TD. As the basal slip showed the lowest CRSS value, it was the easiest to be activated. However, the basal slip could not satisfy the deformation requirement, so the prismatic or pyramidal slip was activated. Because of their high critical stresses, a greater external force was required to cause the yielding behavior, and eventually manifested as an increase in yield stress, which was consistent with results in the literature [22−24].

In terms of elongation, the variation of elongation was more obvious than in the tensile strength along RD. The uniform elongation (UE) along the RD gradually increased from 10.1% (initial) to 12% (Pass 3), while the fracture elongation (FE) increased from 14.6% to 19.1% (Pass 2), and then decreased to 16.3% (Pass 3). The increase of UE along the RD was related to the weakening of basal texture. In the magnesium alloy with weak basal texture, ⟨a⟩ dislocation cross-slip migration from the basal to the prismatic would be limited, resulting in weakened dynamic recovery and enhanced strain hardening, thus exhibiting high uniform elongation [25,26].

In order to clearly describe the mechanical behavior, the deformation mechanism was analyzed by the Kocks−Mecking model [27]. The model has been widely used in the analysis of the hardening behavior of magnesium alloys [28,29]. And this model has been applied previously to establishing the relationship between the dynamic response of strain-hardening (Stage III) and grain size and texture. The results showed that the slope of the hardening curve in Stage III was determined by the texture and tended to flatten with the weakening of the basal texture. In this work, the $d\sigma/d\varepsilon$–$(\sigma-\sigma_{0.2})$ curve was used to explore the strain-hardening behavior during tensile deformation, as shown in Fig. 10.

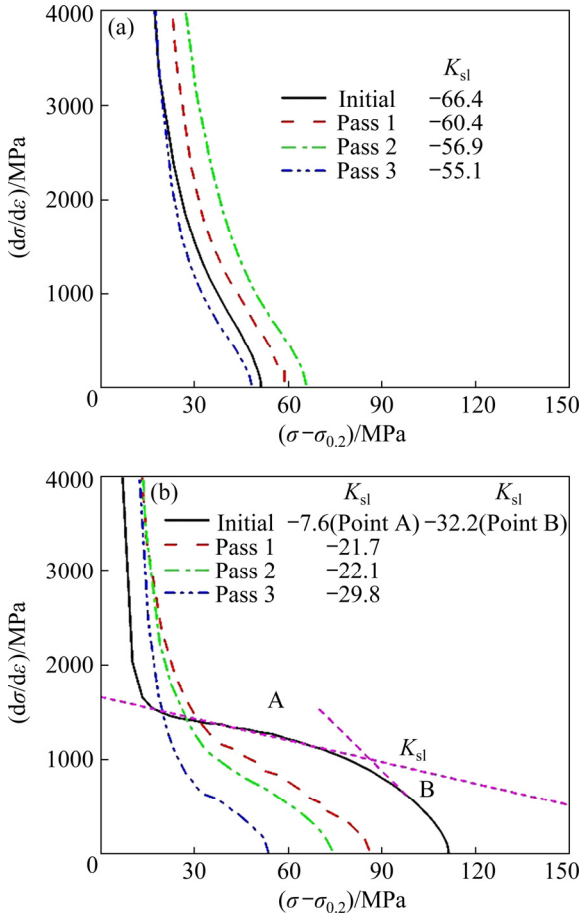

Fig. 10 Strain hardening curves of ZK60 magnesium alloy sheets during asymmetric lowered-temperature rolling: (a) RD; (b) TD

The slope of the hardening curve in Fig. 10 became flatter with weakening of the basal texture, indicating that the slop of hard-working (K_{sl}) value was inversely proportional to the intensity of the basal texture [30,31]. As shown in Fig. 10, K_{sl} was negative in both RD and TD, suggesting that the deformation mechanism was dominated by slip. In addition, with the increase of rolling passes, the value of K_{sl} of the RD gradually increased, indicating that the basal texture along the RD gradually weakened, and the value of K_{sl} of the TD decreased significantly from the initial material to the Pass 1. However, the differences in K_{sl} values between the rolled sheets were minimal, which corresponded with the variation in their texture.

Figure 10 showed that the K_{sl} gradually decreased with the increase of strain. By taking the initial sheet along the TD as an example, the value of K_{sl} decreased from −7.6 (Point A) to −32.2 (Point B), which is closely related to the grain rotation in the tensile process. The initial material texture characteristics suggested that both basal slip and tensile twinning were possible to activate to coordinate tensile deformation along the TD. For grains suitable for basal slip, the basal plane gradually transformed from a soft orientation to a hard orientation under tensile forces. For grains suitable for tensile twinning, tensile twinning activation caused a rotation of 86.3° of the *c*-axis of the grain, and the grain transformed to a hard orientation more quickly [32]. It can be observed that both deformation mechanisms under tensile forces caused the grain orientation to transform into a hard orientation, leading to the basal texture strengthening of the samples, which eventually led to a continuous reduction in the work hardening rate.

4 Conclusions

(1) The asymmetric lowered-temperature rolling reduced the thickness of ZK60 magnesium alloys from 10 to 2.1 mm by three passes, and efficiently refined the average grain size from 26.4 to 7.26 μm. The results showed that ZK60 magnesium alloy sheets with fine grain, and homogeneous microstructure were successfully fabricated by asymmetric lowered-temperature rolling.

(2) The basal texture was transformed from a nearly single-crystal texture in the initial material to a fiber texture by asymmetric lowered-temperature rolling. And asymmetric lowered-temperature rolling rotated *c*-axis of the grain toward the RD by introducing shear, which relatively weakened the basal texture along the RD.

(3) The yield strength of the rolled sheets increased gradually from 157 to 216 MPa due to the effect of grain refinement and increased prismatic slip along the TD. However, the yield strength variation was less along the RD due to the continued weakening of the basal texture along the RD increasing the activation fraction of the basal slip, which counteracted the strengthening effect contributed by the grain refinement. In addition, the weak basal texture was beneficial to increasing the strain hardening rate of the sheet, but the strain hardening rate would decrease due to the change of grain orientation to hard orientation during the tensile process.

Acknowledgments

This work was supported by the National Natural Science Foundation of China (Nos. 51975146, 51801192, 52205344), the Natural Science Foundation of Shandong Province, China (No. ZR2020QE171), Key Research and Development Plan in Shandong Province, China (No. 2019JZZY010364), and the National Defense Basic Scientific Research of China (No. JCK2018603C017).

References

[1] FERESHTEH S F, FAKHAR N, KARAMI F, MAHMUDI R. Superior ductility and strength enhancement of ZK60 magnesium sheets processed by a combination of repeated upsetting and forward extrusion [J]. Materials Science and Engineering A, 2016, 673: 450−457. https://doi.org/10.1016/j.msea.2016.07.025.

[2] MORDIKE B L, EBERT T. Magnesium: Properties−applications−potential [J]. Materials Science and Engineering A, 2001, 302: 37−45. https://doi.org/10.1016/S0921-5093(00)01351-4.

[3] ZHANG J H, LIU S J, WU R Z, HOU L G, ZHANG M L. Recent developments in high-strength Mg−RE-based alloys: Focusing on Mg−Gd and Mg−Y systems [J]. Journal of Magnesium and Alloys, 2018, 6(3): 277−291. https://doi.org/10.1016/j.jma.2018.08.001.

[4] SOMEKAWA H, KINOSHITA A, WASHIO K, KATO A. Enhancement of room temperature stretch formability via grain boundary sliding in magnesium alloy [J]. Materials Science and Engineering A, 2016, 676: 427−433. https://doi.org/10.1016/j.msea.2016.09.014.

[5] ZHOU Yi-yuan, FU Peng-huai, PENG Li-ming, WANG Dan, WANG Ying-xin, HU Bin, LIU Ming, SACHDEV A K, DING Wen-jiang. Precipitation modification in cast Mg−1Nd−1Ce−Zr alloy by Zn addition [J]. Journal of Magnesium and Alloys, 2019, 7(1): 113−123. https://doi.org/10.1016/j.jma.2019.02.003.

[6] XIE Jin-shu, ZHANG Jing-huai, YOU Zi-hao, LIU Shu-juan, GUAN Kai, WU Rui-zhi, WANG Jun, FENG Jing. Towards developing Mg alloys with simultaneously improved strength and corrosion resistance via RE alloying [J]. Journal of Magnesium and Alloys, 2021, 9(1): 41−56. https://doi.org/10.1016/j.jma.2020.08.016.

[7] HAN K, BOHLEN J, WENDT J, KAINER K U, YI S B, LETZIG D. Effect of rare earth additions on microstructure and texture development of magnesium alloy sheets [J]. Scripta Materialia, 2010, 63(7): 725−730. https://doi.org/10.1016/j.scriptamat.2009.12.033.

[8] YANG Zhe-quan, MA Ai-bin, LIU Han, SONG Dan, WU Yu-na, YUAN Yu-chun. Managing strength and ductility in AZ91 magnesium alloy through ECAP combined with prior and post aging treatment [J]. Materials Characterization, 2019, 152: 213−222. https://doi.org/10.1016/j.matchar.2019.04.022.

[9] ZHANG Hua, REN Shuai, LI Xia, WANG Li-fei, FAN Jian-feng, CHEN Shu-ying. Dramatically enhanced stamping formability of Mg−3Al−1Zn alloy by weakening (0001) basal texture [J]. Journal of Materials Research and Technology, 2020, 9(6): 14742−14753. https://doi.org/10.1016/j.jmrt.2020.10.041.

[10] DAN Luo, WANG Hui-yuan, ZHAO Li-guo, WANG Chen, LIU Guo-jun, LIU Yan. Effect of differential speed rolling on the room and elevated temperature tensile properties of rolled AZ31 Mg alloy sheets [J]. Materials Characterization, 2017, 124: 223−228. https://doi.org/10.1016/j.matchar.2016.12.007.

[11] KIM W J, LEE J B, KIM W Y, JEONG H T, JEONG H G. Microstructure and mechanical properties of Mg−Al−Zn alloy sheets severely deformed by asymmetrical rolling [J]. Scripta Materialia, 2007, 56(4): 309−312. https://doi.org/10.1016/j.scriptamat.2006.09.034.

[12] GONG X, KANG S B, LI S, CHO J H. Enhanced plasticity of twin-roll cast ZK60 magnesium alloy through differential speed rolling [J]. Materials & Design, 2009, 30(9): 3345−3350. https://doi.org/10.1016/j.matdes.2009.03.040.

[13] CHANG L L, CHO J H, KANG S B. Microstructure and mechanical properties of AM31 magnesium alloys processed by differential speed rolling [J]. Journal of Materials Processing Technology, 2011, 211(9): 1527−1533. https://doi.org/10.1016/j.jmatprotec.2011.04.003.

[14] WANG Wen-ke, CHEN Wen-zhen, ZHANG Wen-conng, CUI Guo-rong, WANG Er-de. Effect of deformation temperature on texture and mechanical properties of ZK60 magnesium alloy sheet rolled by multi-pass lowered-temperature rolling [J]. Materials Science and Engineering A, 2018, 712: 608−615. https://doi.org/10.1016/j.msea.2017.12.024.

[15] OLEG S, RUSTAM K, TAKU S. Dynamic recrystallization based on twinning in coarse grained Mg [J]. Materials Science Forum, 2003, 419/420/421/422: 521−526. https://doi.org/10.4028/www.scientific.net/MSF.419-422.521.

[16] WANG Y N, HUANG J C. Texture analysis in hexagonal materials [J]. Materials Chemistry Physics, 2003, 81(1): 11−26. https://doi.org/10.1016/S0254-0584(03)00168-8.

[17] CHEN Wen-zhen, YU Yang, WANG Xue, WANG Er-de, LIU Z. Optimization of rolling temperature for ZK61 alloy

sheets via microstructure uniformity analysis [J]. Materials Science and Engineering A, 2013, 575: 136−143. https://doi.org/10.1016/j.msea.2013.03.057.

[18] LIU X, JONAS J J, LI L X, ZHU B W. Flow softening, twinning and dynamic recrystallization in AZ31 magnesium [J]. Materials Science and Engineering A, 2013, 583: 242−253.

[19] BARNET M R. A Taylor model based description of the proof stress of magnesium AZ31 during hot working [J]. Metallurgical and Materials Transactions A, 2003, 34(9): 1799−1806. https://doi.org/10.1007/s11661-003-0146-5.

[20] GUAN B, XIN YUN C, HUANG X Y, WU P D, LIU Q. Quantitative prediction of texture effect on Hall–Petch slope for magnesium alloys [J]. Acta Materialia, 2019, 173: 142−152. https://doi.org/10.1016/j.actamat.2019.05.016.

[21] DEL V J A, RUANO O A. Influence of the grain size on the strain rate sensitivity in an Mg−Al−Zn alloy at moderate temperatures [J]. Scripta Materialia, 2006, 55(9): 775−778. https://doi.org/10.1016/j.scriptamat.2006.07.013.

[22] SHOU Hao-ge, ZHANG Jia-feng, ZHANG Yong-fa, LONG Da, RAO Jing-song, LIU Qing. Quasi-in-situ analysis of dependency of deformation mechanism and work-hardening behavior on texture in Mg−2Zn−0.1Ca alloy [J]. Journal of Alloys and Compounds, 2019, 784: 1187−1197. https://doi.org/10.1016/j.jallcom.2019.01.159.

[23] WANG Y, CHOO H. Influence of texture on Hall–Petch relationships in an Mg alloy [J]. Acta Materialia, 2014, 81: 83−97. https://doi.org/10.1016/j.actamat.2014.08.023.

[24] WANG Wen-ke, CHEN Wen-zhen, ZHANG Wen-cong, CUI Guo-rong, WANG Er-de. Effect of deformation temperature on texture and mechanical properties of ZK60 magnesium alloy sheet rolled by multi-pass lowered-temperature rolling [J]. Materials Science and Engineering A, 2018, 712: 608−615. https://doi.org/10.1016/j.msea.2017.12.024.

[25] DEL V J A, CARRENO F, RUANO O A. Influence of texture and grain size on work hardening and ductility in magnesium-based alloys processed by ECAP and rolling [J]. Acta Materialia, 2006, 54(16): 4247−4259. https://doi.org/10.1016/j.actamat.2006.05.018.

[26] SONG Bo, XIN Ren-hong, LIAO Ai-lin, YU Wen-bin, LIU Qing. Enhancing stretch formability of rolled Mg sheets by pre-inducing contraction twins and recrystallization annealing [J]. Materials Science and Engineering A, 2015, 627: 369−373. https://doi.org/10.1016/j.msea.2015.01.027.

[27] KOCKS U F, MECKING H. Physics and phenomenology of strain hardening: the FCC case [J]. Progress in Materials Science, 2003, 48(3): 171−273. https://doi.org/10.1016/S0079-6425(02)00003-8.

[28] LOU X Y, LI M, BOGER R K, AGNEW S R, WAGONER R H. Hardening evolution of AZ31B Mg sheet [J]. International Journal of Plasticity, 2007, 23(1): 44−86. https://doi.org/10.1016/j.ijplas.2006.03.005.

[29] KNEZEVIC M, LEVINSON A, HARRIS R, MISHRA R K, DOHERTY R D, KALIDINDI S R. Deformation twinning in AZ31: Influence on strain hardening and texture evolution [J]. Acta Materialia, 2010, 58: 6230−6342. https://doi.org/10.1016/j.actamat.2010.07.041.

[30] ZHANG Li-xin, CHEN Wen-zhen, ZHANG Wen-cong, WANG Wen-ke, WANG Er-de. Microstructure and mechanical properties of thin ZK61 magnesium alloy sheets by extrusion and multi–pass rolling with lowered temperature [J]. Journal of Materials Processing Technology, 2016, 237: 65−74. https://doi.org/1.1016/j.jmatprotec.2016.06.005。

[31] CHEN Wen-zhen, WANG Xue, KYALO M N, WANG Er-de, LIU Z Y. Yield strength behavior for rolled magnesium alloy sheets with texture variation [J]. Materials Science and Engineering A, 2013, 580: 77−82. https://doi.org/10.1016/j.msea.2013.04.120。

[32] ZHU S Q, RINGER S P. On the role of twinning and stacking faults on the crystal plasticity and grain refinement in magnesium alloys [J]. Acta Materialia, 2018, 144: 365−375. https:// doi.org/10.1016/j.actamat.2017.11.004.

ZK60 镁合金异步降温轧制显微组织与力学性能的演变

张文丛，刘欣彤，马俊飞，王文珂，陈文振，刘宇轩，杨建雷

哈尔滨工业大学(威海) 材料科学与工程学院，威海 264209

摘　要：将异步降温轧制应用于制造沿轧制方向具有弱基面织构的细晶 ZK60 镁合金板。结果表明，多道次降温轧制可以显著改善显微结构的均匀性，细化晶粒尺寸。同时，在轧制过程中逐渐形成沿横向的纤维织构。重要的是，沿轧向的剪切变形使基面的 c 轴向轧向旋转，削弱沿此方向的基面织构。受这种显微结构变化的影响，由于连续的晶粒细化和柱面滑移的增加，沿横向的屈服强度持续增加，而由于应变硬化能力的下降，均匀伸长率下降。相反，沿轧向的基面织构的持续减弱大大抵消晶粒细化所带来的强化效果，从而导致屈服强度的轻微下降。

关键词：轧制；异步轧制；晶粒尺寸；织构；屈服强度

(Edited by Bing YANG)